Quantitative Elastohydrodynamic Film Forming for a Gear Oil with Complex Shear-Thinning

Revised June, 2015. Changes in red.

Scott Bair*
Regents' Researcher
Georgia Institute of Technology, Center for High-Pressure Rheology
George W. Woodruff School of Mechanical Engineering
Atlanta, GA 30332-0405, USA
scott.bair@me.gatech.edu

Wassim Habchi
Department of Industrial and Mechanical Engineering, Lebanese American University
Byblos, Lebanon
wassim.habchi@lau.edu.lb

Petr Sperka and Martin Hartl
Faculty of Mechanical Engineering
Brno University of Technology
61669, Brno, Czech Republic
sperka@fme.vutbr.cz,

*Corresponding Author

Abstract

Perhaps the most thorough characterization of the elevated pressure properties of any commercial EHL lubricant is presented here for a gear oil. Compressibility, thermal conductivity and low-shear viscosity were measured. Of particular interest is the shear dependence of viscosity, measured across four decades of stress, which shows two transitions each with a specific value of power-law exponent. An attempt to capture a suspected third transition at very high stress resulted in mechanical degradation of the liquid in the viscometer. Numerical simulations of a point contact between a steel ball and a glass disc showed good agreement over a range of slide-to-roll ratio for the measured central thickness. The agreement for the minimum thickness was excellent. A new result is that shear-thinning of a higher molecular weight component that occurs from 3 to 200 kPa had little effect on the film thickness and could therefore be neglected in a film thickness calculation.

KEYWORDS: elastohydrodynamic, film thickness, EHL, rheology, shear-thinning, compressibility

1. INTRODUCTION

The field of elastohydrodynamic lubrication (EHL) has now diverged into two very separate areas. The first is the classical approach in which primary measurements of liquid properties are not welcomed because these are the properties which must be adjusted to match theory to experiment [1]. The second is the quantitative approach [2] in which primary measurements of liquid properties are essential since these properties are used to predict new contact behavior and validate theory. The quantitative approach has resulted in rapid advances in understanding of film thickness [3-7] and friction [3, 8-11].

There has been recent resurgence of interest in friction of EHL films. Sometimes lost in the discussion is the fact that superposition instructs that the constitutive behavior, which applies to the Hertz zone where friction is generated, must also be applied in the inlet zone where the film is formed. Therefore, it is not sensible or possible to discuss the effect of rheology on friction without addressing the effect on film thickness.

Film thickness is important to the durability of machine components, particularly the minimum value, and the central thickness of the lubricant film determines the shear rate which must be known to calculate friction.

The shear-dependent viscosity, η, of multigrade crankcase oils most often begins to depart from the low-shear viscosity, μ, at low shear stress and, after a small decrease in viscosity, there is an inflection in the log-log representation of viscosity versus shear stress or rate. The inflection may be followed by a plateau of constant viscosity with a second Newtonian value, μ_2; however, more often, before the viscosity can become constant, the shear dependence of the base oil begins to affect the overall viscosity. See Figure 1 for an example from [12] of a 10W-40 motor oil. This behavior can be accurately described within a limited range of shear stress, τ, by a multi-component modified Carreau (MCMC) equation introduced by Bair and coworkers [13] in 2005.

$$\eta = \mu \sum_{i=1}^{N} f_i \left[1 + \left| \frac{\tau}{G_i} \right|^2 \right]^{\frac{\left(1-\frac{1}{n_i}\right)}{2}}, \quad \sum_{i=1}^{N} f_i = 1 \qquad (1)$$

The parameters of this model are listed in Table 1 for several commercial lubricants.

The shear response of a multigrade gear oil is usually different. The shear-thinning begins at greater shear stress and the inflection is seldom seen as there is a smaller interval between the first Newtonian limit, G_1, and the shear thinning of the base oil, G_2. An example for a 75W-90 gear oil is included in Figure 1 from [14] to illustrate the difference. Parameters are listed in Table 1.

In this article, the properties of a commercial high viscosity gear oil, Mobilgear SHC 6800, are thoroughly characterized for a film thickness calculation. This oil is the middle viscosity grade of a series of five gear oils (1500, 3200, 6800, 22M and 46M) by the same manufacturer. The high viscosity is beneficial for measurement of the shear dependent viscosity since pressures need not be extreme to generate large shear stress. Shear-thinning models which can be useful in EHL simulations of gear contacts are evaluated. The central and minimum film thicknesses predicted from the measured properties are compared with accurate film thickness measurements. Data such as these should also be useful in accurately predicting friction provided that the stress is sufficiently low to avoid degradation.

2. COMPRESSIBILITY

The change in length of a metal bellows can be measured by a potentiometer housed within a pressure vessel to detect changes in volume of a liquid [15]. The maximum pressure is 400 MPa and the temperature goes to 110°C. The sample volume may not be less than 0.84 of the volume captured when the sample was installed at ambient temperature and pressure. Also, the volume must not exceed 1.09 of the volume captured when the sample was installed or the bellows will be permanently deformed. There is no known viscosity limit for the potentiometer-based instrument and for this reason it is employed here. The relative volume calibrations were

performed with water using the National Institute for Standards and Technology certified densities [16].

The relative volumes, $V/V_R = V(T, p)/V\left(T_R = 30^{\circ}\mathrm{C}, p = 0\right)$, of the oil referenced to 30°C and atmospheric pressure are listed in Table 2. The Murnaghan equation of state [17] is used to represent the temperature and pressure dependence of the density of the gear oil. It reads

$$\frac{V}{V_0} = \frac{\rho_0}{\rho} = \left(1 + \frac{K_0'}{K_0} p\right)^{\left(-\frac{1}{K_0'}\right)} \qquad (2)$$

The isothermal bulk modulus for this model is $K = K_0 + K_0' p$.

For any isothermal form, $K_0(T)$ can be described by

$$K_0 = K_{00} \exp\left(-\beta_K T\right) \quad (3)$$

V_0 must also vary with temperature and a linear dependence of ambient pressure density on temperature is most often employed; however such a relationship will sometimes lead to crossing of isotherms. To avoid this difficulty the ambient pressure volume is made linear with temperature.

$$\frac{V_0}{V_R} = 1 + a_V \left(T - T_R\right) \quad (4)$$

Here V_R is the reference volume at the reference temperature, $T_R = 30\ ^{\circ}\mathrm{C}$ and ambient pressure. The parameters of equations (2-4) are listed in Table 3. This correlation is compared to the data and to a comercial 85W-140 gear oil in Figure 2.

3. THERMAL CONDUCTIVITY

The thermal conductivity at ambient pressure, k_0, was measured by transient hot-wire technique at 30 and 50°C, giving 0.146 and 0.139 W/mK, respectively, with estimated uncertainty of 0.002 W/mK. With k_R =0.146 W/mK and $a_k = -0.0025\ \mathrm{K}^{-1}$, the ambient pressure conductivity can be given [18] as

$$k_0(T) = k_R\left[1 + a_k(T - T_R)\right] \quad (5)$$

A simple density scaling rule for the thermal conductivity at elevated pressure [19] is assumed to hold here.

$$k(T,p) = k_0(T)\left(\frac{\rho(T,p)}{\rho_0(T)}\right)^3 = k_0(T)\left(\frac{V(T,p)}{V_0(T)}\right)^{-3} \quad (6)$$

4. LIMITING LOW-SHEAR VISCOSITY

A falling cylinder viscometer [20] was used to determine the viscosity as a function of pressure. Because of the low shear stress, 45 Pa, used in these stress-controlled measurements, the viscosity may be considered to be the limiting-low-shear viscosity, μ. The estimated uncertainties are 3% for viscosity, 0.5°C for temperature and the greater of 1MPa and 0.5% in pressure for pressures to 350 MPa and 0.7 % for pressures above 350 MPa. The results are listed in Table 4.

At least eight different definitions of the pressure-viscosity coefficient have been used. The reciprocal asymptomatic isoviscous pressure coefficient,

$$\alpha = \left[\int_0^\infty \frac{\mu(p=0)}{\mu(p)}dp\right]^{-1} \quad (7)$$

is the coefficient employed in the Hamrock and Dowson film thickness formulas and is given here in Table 4. There is no consensus on the proper definition of the pressure-viscosity coefficient for film forming.

The Yasutomi model [21], which does not require an equation of state, is a pressure modification of the Williams-Landel-Ferry [22] model for the temperature dependence of the dynamic properties of super-cooled liquids

$$\mu = \mu_g \exp\left[\frac{-2.303C_1(T - T_g)F}{C_2 + (T - T_g)F}\right] \quad (8)$$

where $T_g(p)$ is the glass transition temperature which varies with pressure as

$$T_g = T_{g0} + A_1 \ln(1 + A_2 p) \quad (9)$$

The dimensionless relative thermal expansivity of the free volume, $F(p)$, is given by a new empirical expression [23].

$$F = (1 + b_1 p)^{b_2} \qquad (10)$$

The glass viscosity, μ_g, was assumed to have the "universal" value of 10^{12} Pa·s. Additional parameters are listed in Table 5. The viscosities near ambient pressure are quite important to film forming. Due to the relative importance of the low pressures, the data at 0.1, 25 and 50 MPa were weighted at times 16, times 4 and times 2, respectively in the least squares regression. The curves shown on the plot in Figure 3 are the Yasutomi correlation.

The log(viscosity) versus pressure inflection has not been reached in the data. There is no data above the inflection pressure to uniquely define the parameters in the correlation. Therefore extrapolation above the inflection is expected to underestimate the viscosity at high pressures.

5. SHEAR-DEPENDENT VISCOSITY

The pressurized thin-film Couette viscometer has been previously described [15]. The gear oil was sheared between a rotating cylinder and a stationary cylinder immersed in compressed liquid within a pressure vessel. The radial clearance was established by measurements on diisodecyl phthalate (DIDP), (Fluka >99%). DIDP is an internationally recognized reference liquid for high pressure [24] and has pressure and temperature response similar to liquid lubricants.

Three cylinder sets were employed to characterize shear-thinning across four decades of shear stress, six decades considering the falling body measurements. The cylinder sets are described in Table 6. Any experimental measurement of viscosity involves shearing of the liquid which produces an increase in the temperature of the liquid. For measurements of constitutive response, it is necessary that the associated temperature increase does not obscure the change in viscosity due to molecular alignment. That is to say, the product of the temperature increase and the temperature-viscosity coefficient must be small. The temperature-viscosity coefficient is known from the low-shear measurements. There are two sources of temperature increase of the

sheared liquid, the temperature increase at the working surface of the cylinders and the variation of temperature across the film.

To mitigate the temperature increase at the working surface, the cylinders are fabricated from very high thermal conductivity materials and each measurement consists of shearing for a single rotation of the rotating inner cylinder. The highest rotational speed was 2 revolutions per second. The stepper motor was programmed for 10 ms acceleration. The torque transducer damping fluid is Fluorinert FC77 which has such low viscosity at the test pressures that the transducer response time is less than the acceleration time. The method of braking one of two rotating cylinders [25], which produces millisecond response, was not used because high shear rates are not of interest in a shear-thinning measurement when pressure and temperature are variable. To reduce the temperature variation across the film, the shearing films are thin, yielding small values of the Nahme-Griffith number.

Shear dependent viscosities are plotted versus shear stress in Figure 4. Three regimes of shear dependence are observed in the data. First, at shear stress less than 3 kPa, the viscosity is constant. Second, there is mild shear dependence from 3 to 150 kPa. Third, at shear stress greater than 150 kPa, the viscosity is more strongly shear dependent up to the highest measured stress of 5 MPa. The mild shear dependence from 3 to 150 kPa is typical of the response to addition of a polymer viscosity improver [26]. The shear dependence at shear stress greater than 150 kPa has been observed in a high viscosity polyalphaolefin base oil [13].

Following the highest stress applied by the 8 mm diameter cylinder set, 1.4 MPa, the viscosity was repeatable at lower stress. Therefore, it may be assumed that the gear oil does not mechanically degrade at shear stress up to 1.4 MPa, indicating that degradation should not affect film thickness in a glass/steel rolling contact [27]. Degradation was observed at much greater stress and this will be discussed later.

It can be seen from the presentation of viscosity versus shear stress in Figure 4 that, to a good approximation, the flow curves would superimpose by shifting vertically. This is time-temperature-pressure superposition, the means by which shear-thinning can be applied to practical tribology problems. Vertical shifting has been done for the highest and lowest viscosity flow curves in Figure 5 by reducing the generalized viscosity, η, through dividing by the low-shear viscosity, μ. It can be noticed that the vertical shifting in Figure 5 is not perfect. This may be reconciled by setting each value of G proportional to μ^m [26] with $m = 0.09$ here rather

than having each modulus being a constant. This shifting will not bring a noticeable change in a tribological calculation, however.

Three shear-thinning models have been employed here, the multi-component modified Carreau (MCMC) equation (1) with two components (MCMC2) and the multi-component modified Carreau (MCMC) equation (1) with one component (MCMC1) and a new Ree-Eyring-Carreau (REMC) multi-component equation introduced below. These models are shown in Figure 5.

In Figure 5 the MCMC2 model departs from power-law behavior for shear stress greater than about 3 MPa. The first component with the largest value of η_i, 0.873 versus 0.72 for the second, will become dominant at high shear stress. The single component version, MCMC1, eliminates this issue: however, as shown in Figure 5, the contribution of the higher molecular weight constituent to shear-thinning is lost. Because the response is power-law at high stress, the Ree-Eyring-Carreau model below was introduced in reference [28] to maintain power-law behavior at high stress.

$$\eta = \mu\left\{\sum_{i=1}^{N-1}\frac{f_i G_i}{\mu\dot{\gamma}}\sinh^{-1}\left(\frac{\mu\dot{\gamma}}{G_i}\right)+f_N\left[1+\left(\frac{\mu\dot{\gamma}}{G_N}\right)^2\right]^{\frac{n-1}{2}}\right\},\ \sum_{i=1}^{N} f_i = 1,\ \text{and}\ G_N > G_j\ \text{for}\ j<N \qquad (11)$$

The Ree-Eyring equation [29], (11) without the Carreau term, was offered by Eyring and coworkers as a constitutive model to describe power-law response of mixtures. There is an advantage in the use of sinh terms over the Carreau terms for the shear dependence of components with low Newtonian limits. Power-law behavior can be modeled over a small interval of stress as with Carreau; however, the sinh term quickly vanishes at higher stress while the Carreau term of low Newtonian limit components will dominate at very much higher stress. The disadvantage is that more terms are required to give power-law behavior. The Carreau term was added in reference [28] for convenient extrapolation. The preferred independent variable here is stress. Therefore equation (11) was modified in this work to become the Ree-Eyring-modified Carreau (REMC) model used here.

$$\eta = \mu \left\{ \sum_{i=1}^{N-1} \frac{f_i \tau}{G_i \sinh\left(\frac{\tau}{G_i}\right)} + f_N \left[1 + \left| \frac{\tau}{G_N} \right| \right]^{1-\frac{1}{n}} \right\}, \ \sum_{i=1}^{N} f_i = 1, \text{ and } G_N > G_j \text{ for } j < N \qquad (12)$$

The parameters are listed in Table 7 and the reduced viscosity is plotted in Figure 5. Notice that REMC and MCMC1 differ only in the effect of shear-thinning contributed by a high molecular weight constituent and this will be used to investigate its effect on film thickness in what follows.

The shear-thinning relation most often employed in classical EHL, which makes shear rate vary with the hyperbolic sine function of stress, is actually not shear-thinning. It is an empirical equation describing thermal softening due to viscous heating in Poiseuille flow [30], which was mistaken for another form of non-Newtonian flow, thixotropy, in early viscosity measurements [31].

6. EHL FILM THICKNESS CALCULATIONS

The film thickness calculations in this work are done using the thermal generalized-Newtonian EHD model developed by Habchi et al. [32] based on the full-system finite element approach. It consists in solving first the EHD part; that is, the generalized-Reynolds [33], linear elasticity and load balance equations in a fully-coupled fashion. The full-coupling provides any loss of information that would occur in a weak-coupling scheme and would lead to slow convergence properties of the overall numerical procedure. The solution of this part provides the pressure and film thickness distributions in the contact. These are used as input for the thermal part of the problem. The latter consists in applying the heat transfer equation to the lubricant film and contacting solids. The arising equations in the lubricant and solid domains are then also solved in a fully-coupled fashion. This gives rise to an updated temperature field which is used to update the lubricant properties throughout the film. In fact, the employed model accounts for the viscosity, density and thermal conductivity variations of the lubricant with pressure and temperature throughout the film. It also accounts for the variations of viscosity with shear stress. An iterative procedure is established between the EHD and thermal part until both pressure and temperature fields within the contact are converged. All equations are discretized using finite

elements. Being non-linear, these are solved using a Newton-like procedure. For further details about the employed geometries, meshes, solution techniques, etc. the reader is referred to [32].

7. EHL FILM THICKNESS MESUREMENTS

Film thickness measurements were carried out using optical tribometer and colorimetric interferometry technique [34] in improved configuration where a color/film connection is represented by empirically fitted functions and a silica spacer layer is not used [35]. This technique evaluates the film thickness from interferograms by color matching algorithm and color-film thickness calibration curves with nanometer resolution. The calibration curves are obtained from Newton rings for static contact immersed with lubricant. Because these rings are generated at ambient pressure out of highly loaded zone, the calibration does not include change of lubricant refractive index with pressure. Therefore central film thickness data are corrected after color-film thickness evaluation by method based on Lorentz-Lorenz equation [28] and Murnaghan equation (2) for density variation with pressure. The calculated correction factor has decreased the reported central film thickness by 5.4 %. Minimum film thickness is not corrected since pressure in this area is close to ambient pressure.

Elastohydrodynamic contact was formed between glass disc and steel ball giving reduced modulus of elasticity 123.8 GPa. The measurements were conducted for load of 48 N corresponding to 0.6 GPa Hertzian pressure, mean speed of 20 mm/s, slide/roll ratio from 0 to 50% and temperature of 60 ± 0.5°C. Due to high viscosity of gear oil the main part of film thickness measurement uncertainty comes from temperature inaccuracy. For this gear oil at temperature around 60°C the deviation of 0.5 °C corresponds to approximately 6 nm central film thickness change. Hence the tribometer was stabilized for one hour to achieve high uniformity of temperature and all measurements were done in close succession. All simulations and reported measurements are for the case of the ball moving faster than the disc. Film thickness results together with the present calculated values and Hamrock and Dowson [36] isothermal, Newtonian predictions are shown in Figure 6. Calculated data obtained by the numerical solution described in Section 6 are provided for two shear-thinning models.

8. DISCUSSION

Perhaps the most thorough characterization of the elevated pressure properties of any EHL lubricant is presented here. Of particular interest is the shear dependence of viscosity, measured across four decades of stress, which shows two transitions each with a specific value of power-law exponent.

The measurements and calculations of film thickness shown in Figure 6 clearly indicate that the use of measured shear-dependent viscosity improves the prediction of film thickness over the most commonly used film thickness formula. Surprisingly, the agreement is better for the minimum than the central thickness. Of course, adjusting the pressure-viscosity coefficient of the Hamrock and Dowson formula to match the measured film thicknesses, the usual approach in classical EHL, would improve the agreement; however, this would not be a prediction of film thickness and would not be helpful in extrapolating to the more severe conditions of a real gearbox. The scale and load dependence of film thickness are both influenced by the shear-thinning response of the gear oil [5, 6]. We have used the definition of quantitative EHL which was introduced in a letter to the editor of this journal [37]. That letter defines quantitative EHL, as opposed to classical, as using accurately measured viscosity rather than the usual method of adjusting viscosity. The classical approach is the one that gives almost perfect fit to data as the viscosity is adjusted to do so. The quantitative approach may not. New discoveries may result from the lack of a perfect fit when the real viscosity is used.

An interesting aspect of the calculations is that the two models, REMC and MCMC1, which differ only in the effect of shear-thinning contributed by a higher molecular weight constituent, yield nearly the same film thicknesses, REMC being slightly thinner. A previous paper [38] using a very simple calculation identified the important interval of shear stress for film-forming in the glass/steel system to be 100 to 3000 kPa. The two models only diverge for stress less than about 200 kPa in Figure 5, supporting the previous finding. More interesting however is the result that shear-thinning of the higher molecular weight component that occurs from 3 to 200 kPa had little effect on the film thickness and could therefore be neglected.

The oil manufacturer does not fully disclose the formulation except to indicate that the base oil is synthetic hydrocarbon. Therefore gel permeation chromatography was employed to confirm that two very different molecular weight components were responsible for the two

transitions found in the flow curves. The chromatogram (Figure 7) indicated peaks with third moment molecular weights of 17,000 and 1300 Daltons. The first peak is a polymeric thickener and the second is a high viscosity synthetic hydrocarbon base oil. However, there was a third small peak at 500 Daltons that is believed to be a polar liquid used for solvency. The molecular weights at the peaks are indicated in Figure 7. This motivated a search for a third transition in the shear dependence at still greater stress.

Another viscometer was used to characterize the shear dependence for shear stress greater than 6 MPa in the search for a third transition. This viscometer was designed to measure viscosity at the very high shear stress required to characterize shear thinning in low molecular weight base oils [15]. The gear oil was sheared at $\dot{\gamma} = 400$ s^{-1} at 23°C with the pressure set to 400 MPa for three revolutions to center the cylinder set using the normal stress effect [39]. The stress should have been $\tau = 9$ MPa from equation (12). A stress peak was observed followed by a decrease over three revolutions. Subsequent attempts at a steady single revolution measurement resulted in progressively lower stress. This is mechanical degradation [15]. Mechanical degradation of the liquid will certainly be a problem for any attempt to calculate friction at high shear stress. Simulation of an EHL film with mechanical degradation of the liquid requires that the stress history of each liquid particle be tracked [40] and is one of the most challenging issues in EHL.

9. CONCLUSION

A commercial gear oil was subjected to perhaps the most thorough characterization of the elevated pressure properties of any EHL lubricant. Compressibility, thermal conductivity, low-shear viscosity and shear-dependent viscosity were measured. Shear-dependent viscosity was measured across four decades of stress. Two transitions, each with a specific value of power-law exponent were observed. An attempt to capture a suspected third transition at very high stress resulted in mechanical degradation of the sample in the viscometer. Numerical simulations of a point contact between a steel ball and a glass disc showed good agreement over a range of slide-to-roll ratio for the measured central thicknesses. A new result is that shear-thinning of a higher molecular weight component that occurs from 3 to 200 kPa had little effect on the film thickness and could therefore be neglected in a film thickness calculation.

ACKNOWLEDGMENT

Bair benefited from a conversation with Mark Devlin at Afton Chemical. The authors thank Weixue Tian of Caterpillar Company for distributing samples of the gear oil.

Funding

Bair was supported by the Center for Compact and Efficient Fluid Power, a National Science Foundation Engineering Research Center funded under cooperative agreement number EEC-0540834. Film thickness measurements at Brno University of Technology were carried out with the support of the NETME Centre - Project No. CZ.1.07/2.3.00/30.0005 and Czech Science Foundation - Project No. 15-24091S.

Nomenclature

a_V thermal expansivity defined for volume linear with temperature, K^{-1}

a_k temperature coefficient of k_0, K^{-1}

A_1, A_2, b_1, b_2, C_1, C_2 Yasutomi parameters, various units

f influence fraction

F relative thermal expansivity of the free volume

G effective liquid shear modulus associated with rotational relaxation time, Pa

k liquid thermal conductivity, W/m/K

k_R liquid thermal conductivity at reference state, T_R, $p = 0$, W/m/K

k_0 thermal conductivity at ambient pressure, W/m/K

K_0 isothermal bulk modulus at $p = 0$, Pa

K_0' pressure rate of change of isothermal bulk modulus at $p = 0$

K_{00} K_0 at zero absolute temperature, Pa

m shifting exponent

n power-law exponent

p pressure, Pa

T temperature, K or °C

T_R reference temperature, K or °C

T_g glass transition temperature, K or °C

T_{g0} glass transition temperature at $p = 0$, K or °C

V specific volume at T and p, m^3/kg

V_R specific volume at reference state, T_R, $p = 0$, m^3/kg

V_0 specific volume at $p = 0$, m^3/kg

α reciprocal asymptotic isoviscous pressure coefficient, Pa^{-1}

β_K temperature coefficient of K_0, K^{-1}

$\dot{\gamma}$ shear rate, s^{-1}

η generalized (non-Newtonian) viscosity, $Pa \cdot s$

μ limiting low-shear viscosity, $Pa \cdot s$

μ_g limiting low-shear viscosity at the glass transition, $Pa \cdot s$

ρ mass density, kg/m^3

ρ_0 mass density at $p = 0$, kg/m^3

τ shear stress, Pa

REFERENCES

1. Spikes, H., & Jie, Z. (2014). History, origins and prediction of elastohydrodynamic friction. *Tribology Letters*, *56*(1), 1-25.

2. Bair, S., Vergne, P., Kumar, P., Poll, G., Krupka, I., Hartl, M., Habchi, W. & Larsson, R. (2015). Comment on "History, Origins and Prediction of Elastohydrodynamic Friction" by Spikes and Jie. *Tribology Letters*, *58*(1), 1-8.

3. Liu, Y., Wang, Q. J., Bair, S., & Vergne, P. (2007). A quantitative solution for the full shear-thinning EHL point contact problem including traction. *Tribology Letters*, *28*(2), 171-181.

4. Liu, Y., Wang, Q. J., Krupka, I., Hartl, M., & Bair, S. (2008). The shear-thinning elastohydrodynamic film thickness of a two-component mixture. *Journal of tribology*, *130*(2), 021502.

5. Krupka, I., Bair, S., Kumar, P., Khonsari, M. M., & Hartl, M. (2009). An experimental validation of the recently discovered scale effect in generalized Newtonian EHL. *Tribology letters*, *33*(2), 127-135.

6. Krupka, I., Kumar, P., Bair, S., Khonsari, M. M., & Hartl, M. (2010). The effect of load (pressure) for quantitative EHL film thickness. *Tribology letters*, *37*(3), 613-622.

7. Habchi, W., Bair, S., Qureshi, F., & Covitch, M. (2013). A Film Thickness Correction Formula for Double-Newtonian Shear-Thinning in Rolling EHL Circular Contacts. *Tribology Letters*, *50*(1), 59-66.

8. Habchi, W., Vergne, P., Bair, S., Andersson, O., Eyheramendy, D., & Morales-Espejel, G. E. (2010). Influence of pressure and temperature dependence of thermal properties of a lubricant on the behaviour of circular TEHD contacts. *Tribology International*, *43*(10), 1842-1850.

9. Habchi, W., Bair, S., & Vergne, P. (2013). On friction regimes in quantitative elastohydrodynamics. *Tribology International*, *58*, 107-117.

10. Björling, M., Habchi, W., Bair, S., Larsson, R., & Marklund, P. (2013). Towards the true prediction of ehl friction. *Tribology International*, *66*, 19-26.

11. Björling, M., Habchi, W., Bair, S., Larsson, R., & Marklund, P. (2014). Friction Reduction in Elastohydrodynamic Contacts by Thin-Layer Thermal Insulation. *Tribology Letters*, *53*(2), 477-486.

12. Bair, S. (2015) The First Normal Stress Difference in a Shear-Thinning Motor Oil at Elevated Pressure. accepted by *STLE Tribology Transactions*

13. Bair, S., Vergne, P., & Querry, M. (2005). A unified shear-thinning treatment of both film thickness and traction in EHD. *Tribology Letters*, *18*(2), 145-152.

14. Bair, S., & Khonsari, M. M. (2006). Reynolds equations for common generalized Newtonian models and an approximate Reynolds-Carreau equation. *Proceedings of the Institution of Mechanical Engineers, Part J: Journal of Engineering Tribology*, *220*(4), 365-374.

15. Bair, S. S. (2007). *High pressure rheology for quantitative elastohydrodynamics* (Tribology series Volume 54). Elsevier.

16. Lemmon EW, McLinden MO, Friend DG. Thermophysical Properties of Fluid Systems. In: Linstrom PJ, Mallard WG. editors. NIST Chemistry WebBook, NIST Standard Reference Database Number 69, Gaithersburg MD: National Institute of Standards and Technology. Available from: http://webbook.nist.gov.

17. Murnaghan, F. D. (1944). The compressibility of media under extreme pressures. *Proceedings of the national academy of sciences of the United States of America*, *30*(9), 244-247.

18. Assael, M. J., Charitidou, E., & Karagiannidis, L. (1991). The thermal conductivity of n-hexadecane + ethanol and n-decane + butanol mixtures. *International journal of thermophysics*, *12*(3), 491-500.

19. Bair, S. (2014). Density Scaling of the Thermal Conductivity of a Jet Oil. *Tribology Transactions*, *57*(4), 647-652.

20. Bair, S., & Qureshi, F. (2002). Accurate measurements of pressure-viscosity behavior in lubricants. *Tribology transactions*, *45*(3), 390-396.

21.Yasutomi, S., Bair, S., & Winer, W. O. (1984). An application of a free volume model to lubricant rheology I—dependence of viscosity on temperature and pressure. *Journal of tribology*, *106*(2), 291-302.

22. Williams, M. L., Landel, R. F., & Ferry, J. D. (1955). The temperature dependence of relaxation mechanisms in amorphous polymers and other glass-forming liquids. *Journal of the American Chemical society*, *77*(14), 3701-3707.

23. Bair, S., Mary, C., Bouscharain, N., & Vergne, P. (2013). An improved Yasutomi correlation for viscosity at high pressure. *Proceedings of the Institution of Mechanical Engineers, Part J: Journal of Engineering Tribology*, 227(9), 1056-1060.

24. Paredes, X., Fandiño, O., Comuñas, M. J., Pensado, A. S., & Fernández, J. (2009). Study of the effects of pressure on the viscosity and density of diisodecyl phthalate. *The Journal of Chemical Thermodynamics*, *41*(9), 1007-1015.

25. Bair, S. (1995). Recent developments in high-pressure rheology of lubricants. In The Third Body Concept: Interpretation of Tribolical Phenomena, Proceedings of the 22nd Leeds-Lyon Symposium on Tribology, Lyon, pp. 169–187 (Elsevier, Amsterdam).

26. Bair, S., & Qureshi, F. (2014). Time-Temperature-Pressure Superposition in Polymer Thickened Liquid Lubricants. *Journal of Tribology*, *136*(2), 021505.

27. Krupka, I., Bair, S., Kumar, P., Svoboda, P., & Hartl, M. (2011). Mechanical degradation of the liquid in an operating EHL contact. *Tribology letters*, *41*(1), 191-197.

28. Bair, S. (2009). Rheology and high-pressure models for quantitative elastohydrodynamics. *Proceedings of the Institution of Mechanical Engineers, Part J: Journal of Engineering Tribology*, *223*(4), 617-628.

29. Kim, W. K., Hirai, N., Ree, T., & Eyring, H. (1960). Theory of Non-Newtonian Flow. III. A Method for Analyzing Non-Newtonian Flow Curves. *Journal of Applied Physics*, *31*(2), 358-361.

30. Hersey, M. D., & Zimmer, J. C. (1937). Heat effects in capillary flow at high rates of shear. *Journal of Applied Physics*, *8*(5), 359-363.

31. Hahn, S. J., Ree, T., & Eyring, H. (1959). Flow mechanism of thixotropic substances. *Industrial & Engineering Chemistry*, *51*(7), 856-857.

32. Habchi W., Eyheramendy D., Vergne P. and Morales-Espejel G. – Stabilized Fully-Coupled Finite Elements for Elastohydrodynamic Lubrication Problems, *Advances in Engineering Software*, 2012, vol. 46, pp. 4-18.

33. Yang P. and Wen S. - A Generalized Reynolds Equation for Non-Newtonian Thermal Elastohydrodynamic Lubrication, *ASME Journal of Tribology*, 1990, vol. 112, pp. 631-636.

34. Hartl, M., Krupka, I., & Liska, M. (1997). Differential colorimetry: tool for evaluation of chromatic interference patterns. *Optical Engineering*, *36*(9), 2384-2391.

35. Hartl, M., Krupka, I., Fuis, V., & Liska, M. (2004). Experimental study of lubricant film thickness behavior in the vicinity of real asperities passing through lubricated contact. Tribology transactions, 47(3), 376-385.

36. Hamrock, B. J., & Dowson, D. (1977). Isothermal elastohydrodynamic lubrication of point contacts: part III—fully flooded results. *Journal of Tribology*, *99*(2), 264-275.

37. Bair, S., Fernandez, J., Khonsari, M. M., Krupka, I., Qureshi, F., Vergne, P., & Wang, Q. J. (2009). Letter to the Editor. *Proceedings of the Institution of Mechanical Engineers, Part J: Journal of Engineering Tribology*, *223*(4), i-ii.

38. Bair, S., Qureshi, F., & Kotzalas, M. (2004). The low-shear-stress rheology of a traction fluid and the influence on film thickness. *Proceedings of the Institution of Mechanical Engineers, Part J: Journal of Engineering Tribology*, *218*(2), 95-98.

39. Abdel-Wahab, M., Giesekus, H., & Zidan, M. (1990). A new eccentric-cylinder rheometer. *Rheologica acta*, *29*(1), 16-22.

40. Kudish, I. I., & Airapetyan, R. G. (2004). Lubricants with non-newtonian rheology and their degradation in line contacts. *Journal of tribology*, *126*(1), 112-124.

Table 1. Parameters of the 2005 multi-component modified Carreau (MCMC) equation.

Oil	N	i	f_i	n_i	G_i / kPa	Std. Dev.
10W-40	2	1	0.41	0.62	4.8	6.3%
		2	0.59	0.63	6500	
75W-90	2	1	0.38	0.83	20	-
		2	0.62	0.40	2500	
Mobilgear 6800 MCMC2	2	1	0.484	0.873	3.13	3.2%
		2	0.516	0.72	147	
Mobilgear 6800 MCMC1	1	1	1.000	0.77	65	5.3%
		—	—	—	—	

Table 2. Relative Volumes, $V/V_R = V(T, p)\big/V\left(T_R = 30^{\circ}\mathrm{C}, p = 0\right)$.

p/MPa	30°C	60°C	88°C
0	1.0000	1.0172	1.0377
50	0.9754	0.9906	1.0055
100	0.9563	0.9693	0.9827
200	0.9285	0.9388	0.9488
300	0.9090	0.9175	0.9252
400		0.9006	0.9076

Table 3. Murnaghan parameters

K_0'	10.970
K_{00} / GPa	7.608
β_K / $10^{-3}\mathrm{K}^{-1}$	0.004840
a_V / $10^{-3}{}^{o}\mathrm{C}^{-1}$	0.6401
Std. Dev.	0.068%

Table 4. Low-Shear Viscosity in Pa·s

P / MPa	20.5°C	40°C	70°C
0	36.6	7.95	1.23
25	73.9	15.6	2.33
50	138.3	28.8	3.93
100	424	85.0	10.36
150	1339	229	23.9
200		531	51.9
300			206
400		14750	
600			9115
α / GPa^{-1}	25.7	24.3	21.6

Table 5. Yasutomi parameters

T_{g0} / °C	-97.12
A_1 / °C	225.2
A_2 / GPa^{-1}	0.5200
b_1 / GPa^{-1}	8.527
b_2	-0.2438
C_1	17.84
C_2 / °C	83.39
Std. Dev.	5 %

Table 6. Cylinder Sets employed here

Working Diameter / mm	12.65	8.01	5.02
Working Length / mm	9.68	2.87	1.62
Radial Clearance / μm	3.7	6.1	2.2
Piloted	No	Yes	Yes
Thermal Conductivity / W/mK	322	212	212
Used here for μ / Pa·s	$<10^2$	10^2 to 10^4	$>10^4$

Table 7. Parameters of the Ree-Eyring modified Carreau (REMC) model. Standard Deviation is 4.5%.

i	1	2	3
n	-	-	0.758
G/ kPa	3.20	80	220
f	0.100	0.130	0.77

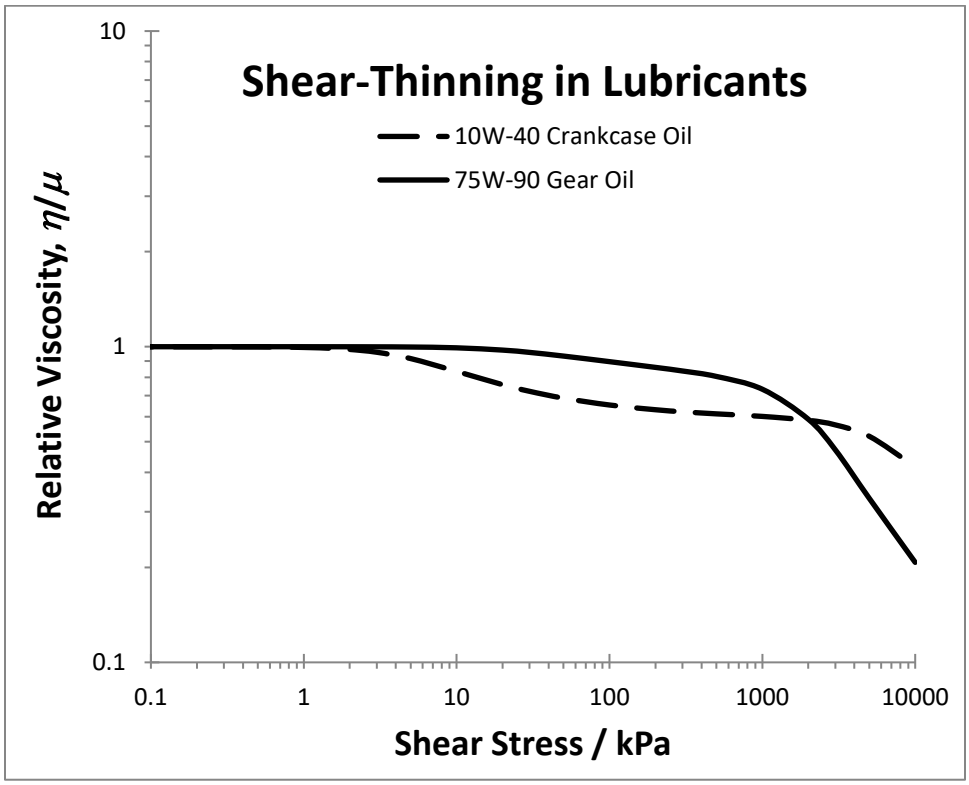

Figure 1. Shear-dependence of viscosity (flow curves) for a crankcase oil and a gear oil showing typical differences.

C:\Users\sb11\Documents\Modeling Data\Mobil 6800\Flow curves for motor vs gear oils.xlsx

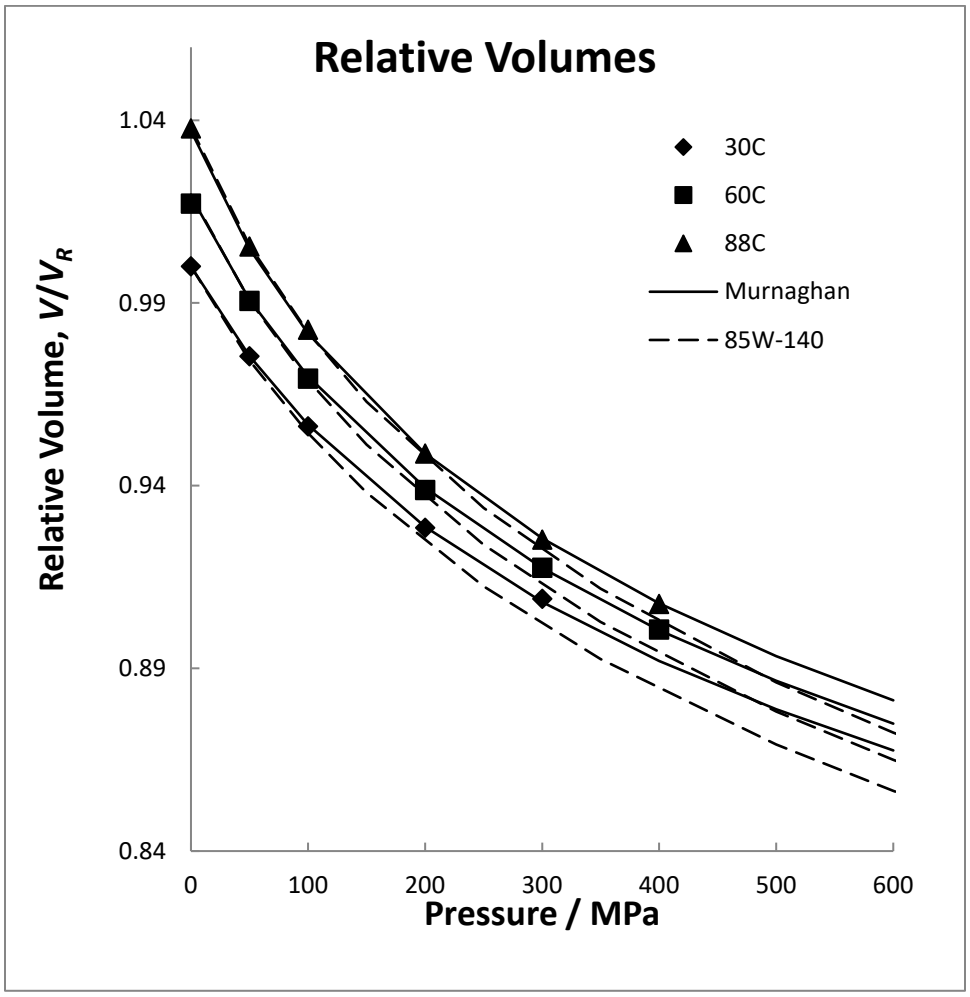

Figure 2. The measured relative volume compared with the Murnaghan equation and an 85W-140 gear oil.

C:\Users\sb11\Documents\Modeling Data\Mobil 6800\Potentiometer based bellows 6800.xlsx

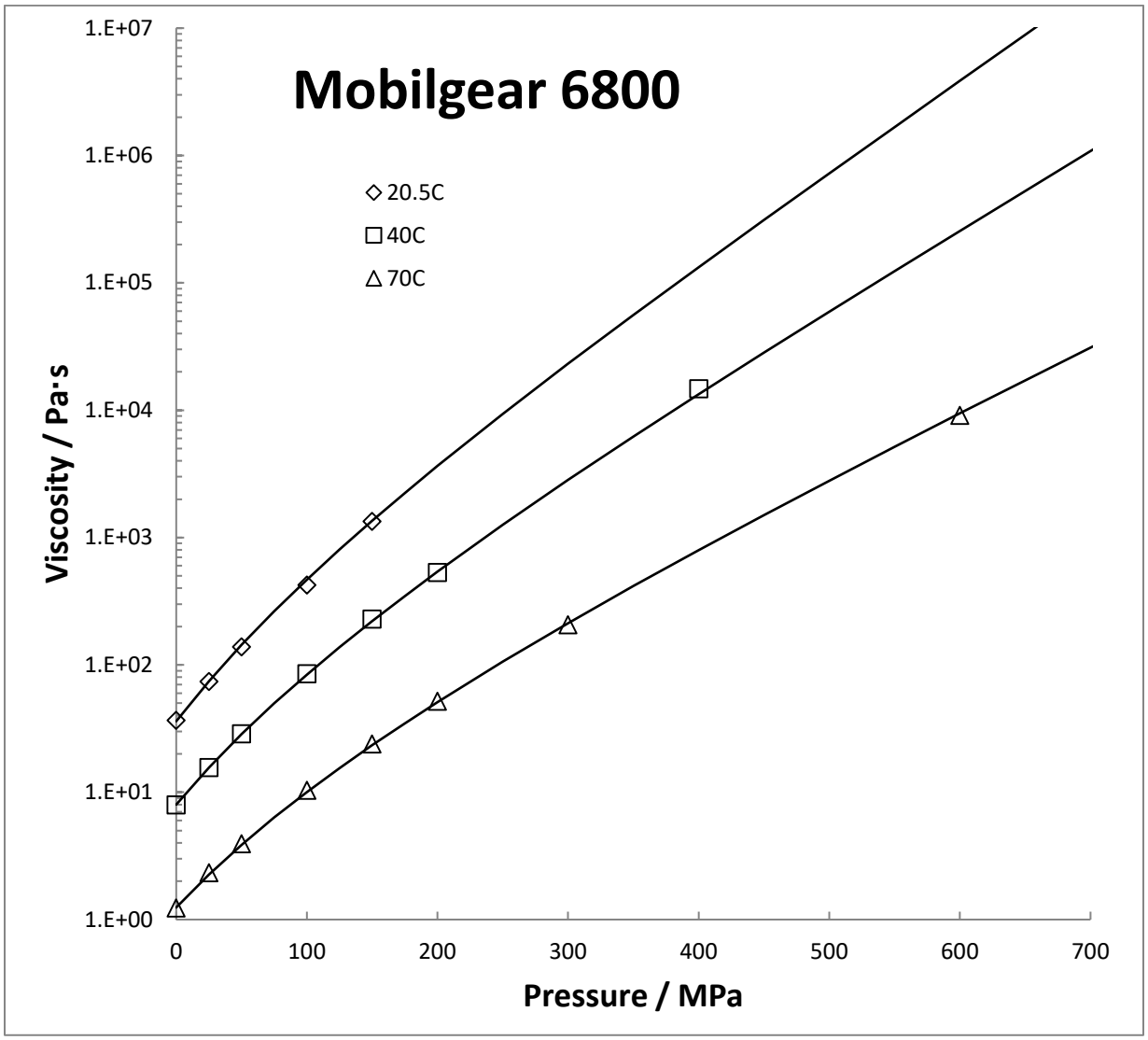

Figure 3. Measured low-shear viscosities and the improved Yasutomi correlation as the curves.

C:\Users\sb11\Documents\Modeling Data\Mobil 6800\Alpha Hollow 6800.xlsx

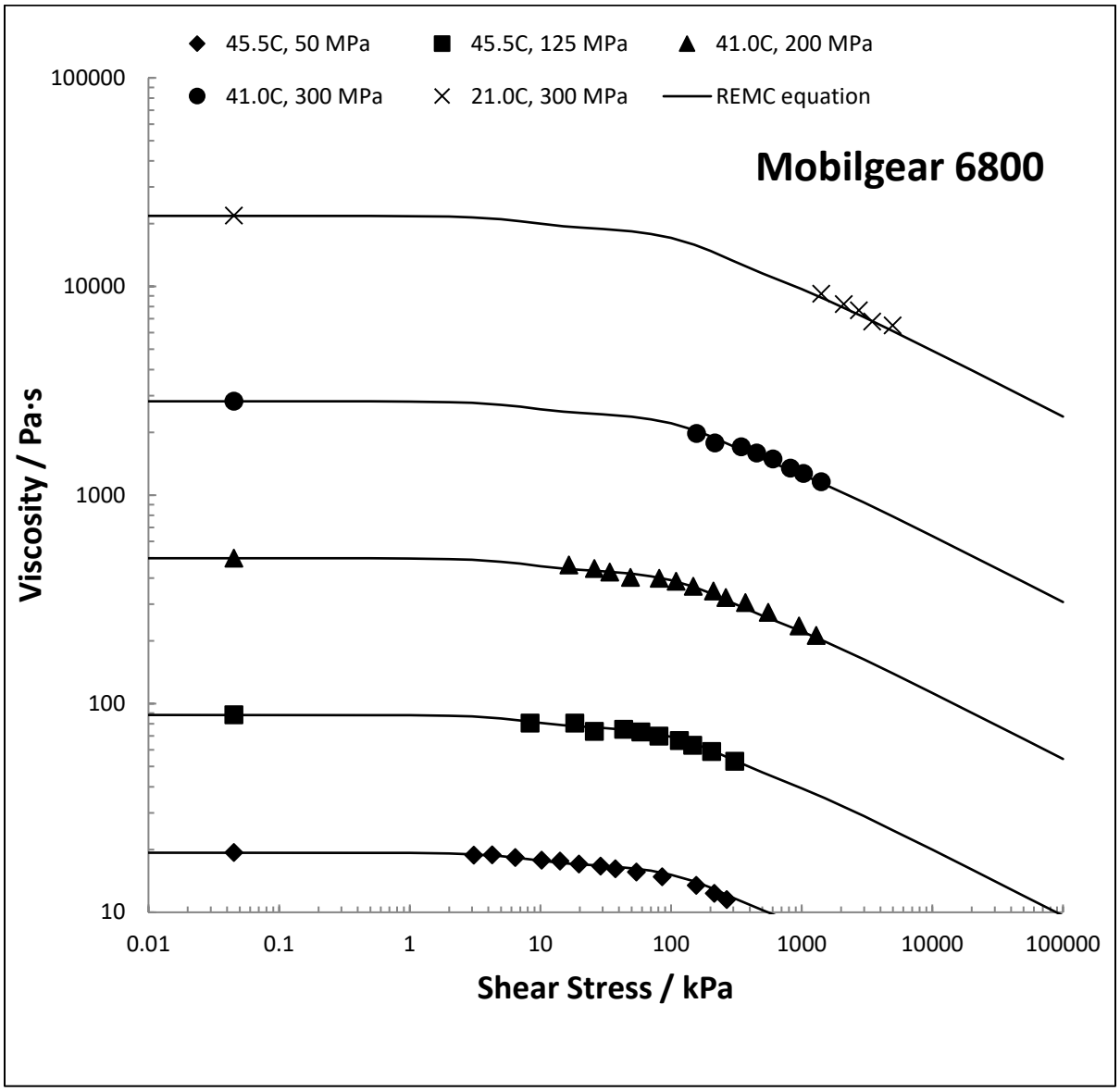

Figure 4. Measured shear-dependent viscosities. Curves are the REMC model.

C:\Users\sb11\Documents\Modeling Data\Mobil 6800\Couette 12#4 6800.xlsx

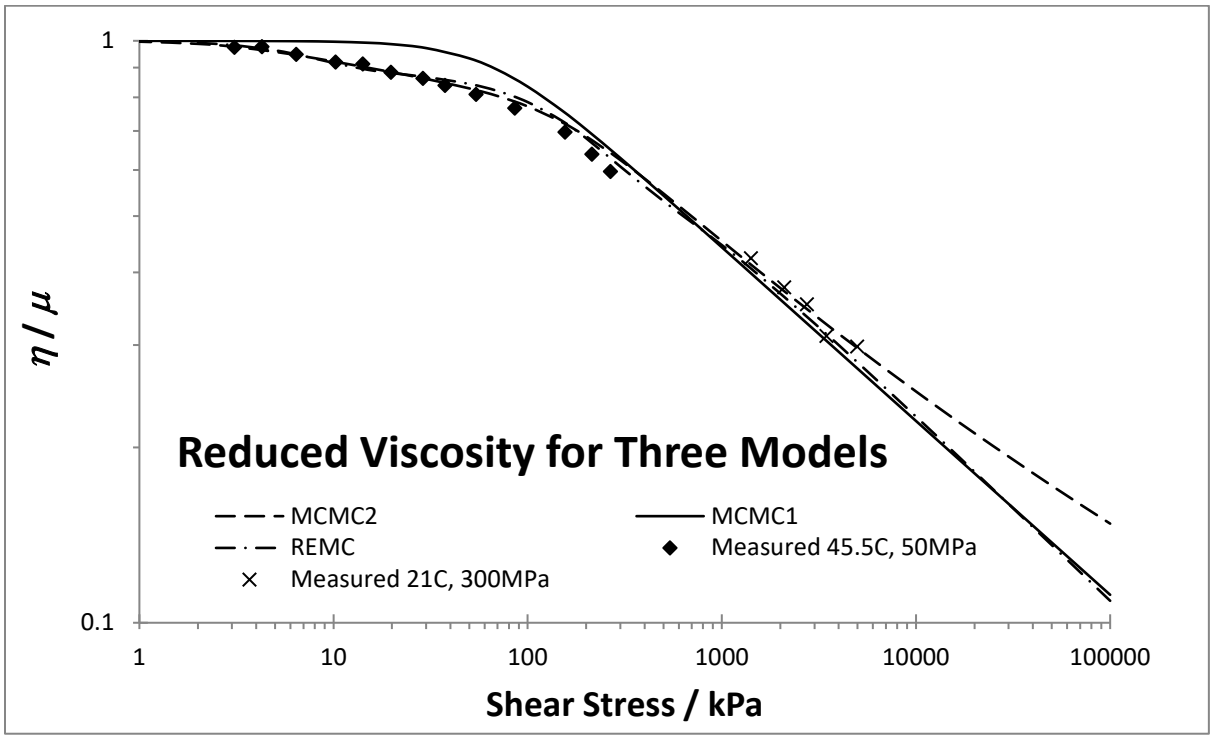

Figure 5. Comparing the MCMC1, MCMC2 and REMC models. MCMC1 eliminates the contribution from the higher molecular weight component.

C:\Users\sb11\Documents\Modeling Data\Mobil 6800\Couette 12#4 6800.xlsx

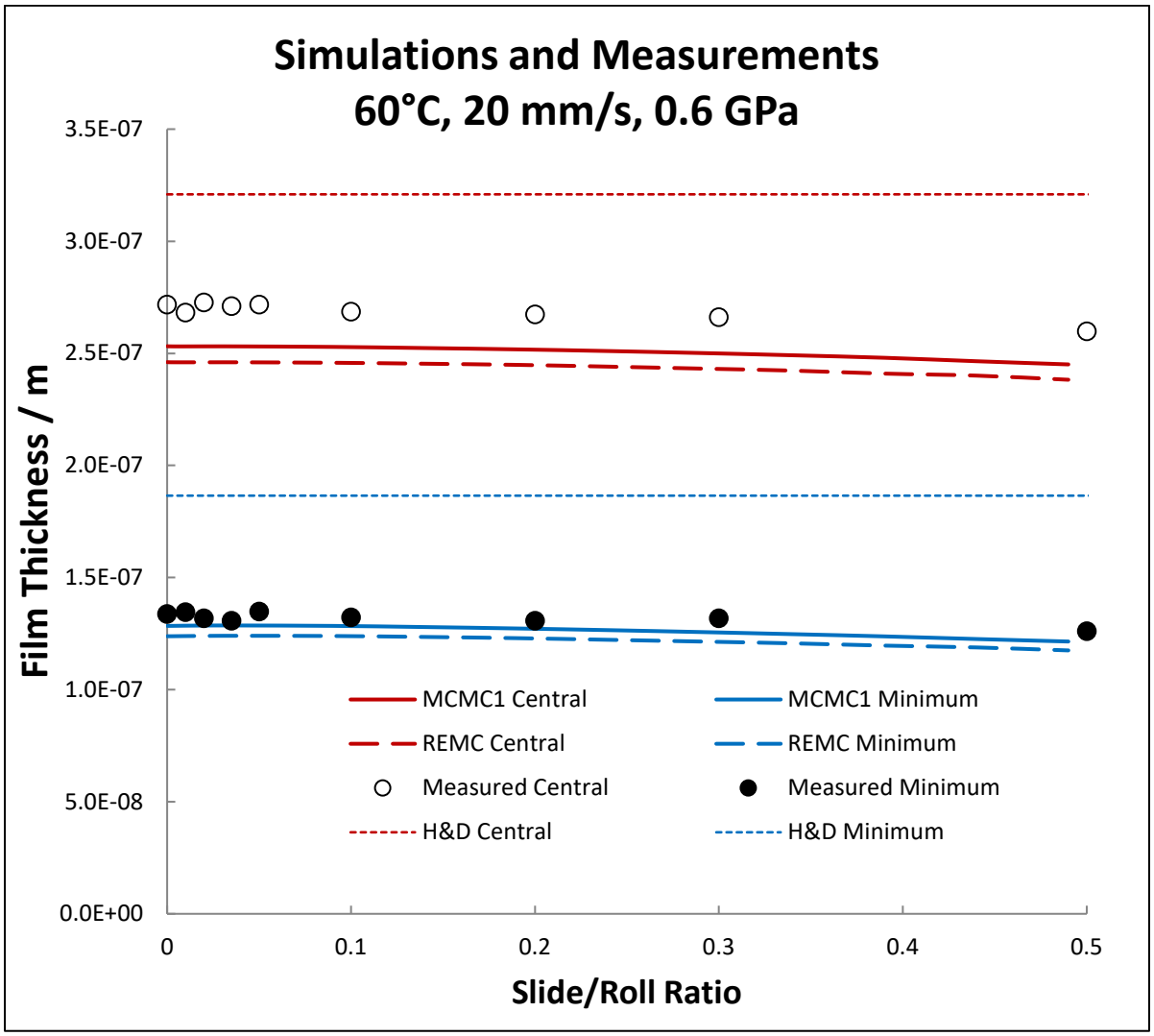

Figure 6. Film thickness measurements(ball moving faster than disk), calculated values and the Hamrock-Dowson isothermal, Newtonian predictions. Calculated curves obtained by the numerical solution described in Section 6 are provided for two shear-thinning models.

C:\Users\sb11\Documents\Papers in progress\Gear Oil\Wassim Results.xlsx

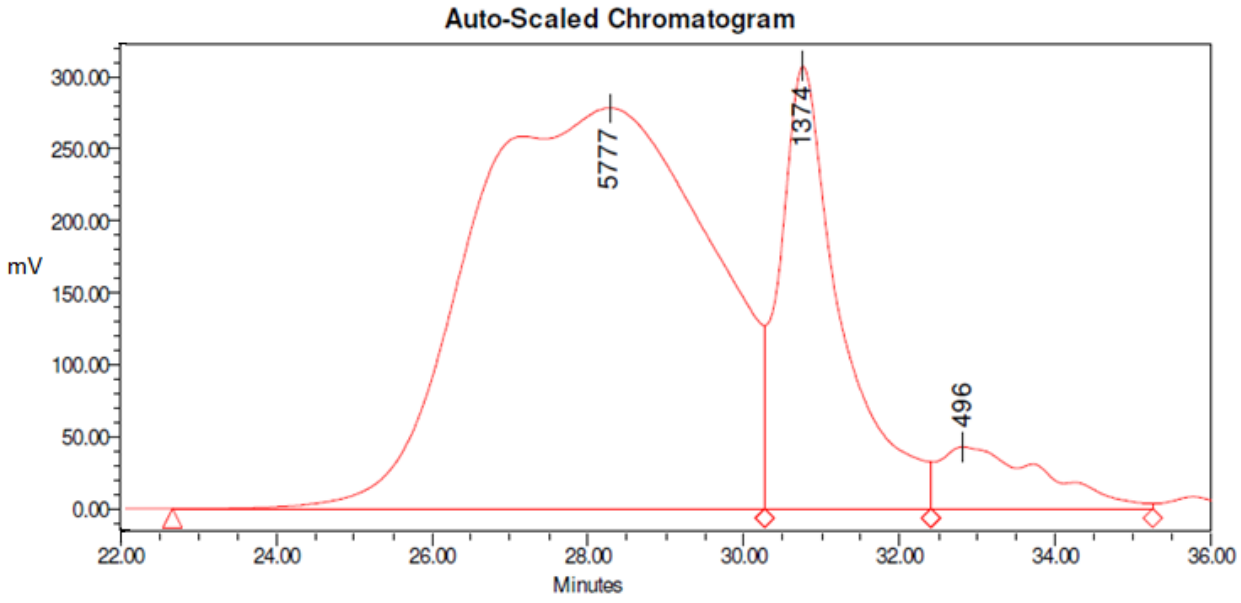

Figure 7. Chromatogram for Mobilgear SHC 6800. Molecular weights at peaks are given in Daltons.

C:\Users\sb11\Documents\Modeling Data GPC2.tiff